NUMERICAL INVESTIGATION ON THE EFFECTS OF SLOTTED HEIGHT ON PERFORMANCE OF LOUVER AND SLIT FINS AT DIFFERENT FIN PITCHES

by

Changshuang ZHI, Xusheng WANG, and Yingwen LIU*

Key Laboratory of Thermo-Fluid Science and Engineering of MOE,
School of Energy and Power Engineering,
Xi'an Jiaotong University, Xi'an, Shaanxi, China

Original scientific paper
https://doi.org/10.2298/TSCI230327147Z

In this paper, the effects of slotted height at different fin pitches are analyzed in detail, aiming to investigate the function and optimal ratio of slotted height to fin pitch. In the cases of high Reynolds number for louver fin, the "bimodal phenomenon" of heat transfer coefficient begins to appear with the increasing slotted height. As the slotted height is about half of the fin pitch, the heat transfer coefficient has a local minimum value, of which there are two peaks on both sides. However, the pressure drop has been increasing with the increasing slotted height. The optimal slotted height under different fin pitches is more instructive than the optimal louver angle. For slit fin, the heat transfer coefficient increases first and then decreases with the increasing slotted height, so does the pressure drop. Meanwhile, as the slotted height is about 0.3~0.45 times and 0.5~0.65 times of fin pitch for louver fin and slit fin, respectively, the comprehensive performance can reach a maximum. The optimal comprehensive performance under 1.2 mm fin pitch is greater than the optimal comprehensive performance under 1.8 mm fin pitch. For lower Reynolds numbers, the optimal comprehensive performance of louver fin is roughly similar to the slit fin. For higher Reynolds numbers, the optimal comprehensive performance of louver fin is greater than that of slit fin.

Key words*: slit fin, louver fin, finned tube heat exchanger, slotted height, fin pitch, air side performance*

Introduction

Finned tube heat exchanger is conspicuous in energy, refrigeration, automobile, microelectronics and other fields. Generally speaking, the finned tube exchanger is composed of round tube and plate fins. The fluid in tube is water or refrigerant, the fluid on the fin side is air [1]. As the thermal resistance on the air side accounts for more than 85% [2], the configuration of plate fin is continuously optimized. Due to the geometric discontinuity, multiple fins can break and renew the boundary-layer and enhance heat transfer [3-5]. Even though louver fin and slit fin are widely used and many researches have been done about the slotted height, there is no unified conclusion that can be generalized to conclude the optimal louver angle or slotted height for different fin pitches.

*Corresponding author, e-mail: ywliu@xjtu.edu.cn

As far as the author knows, the earliest experimental research on louver fins was carried out by Kays and London [6], and the experimental methods and matters needing attention are summarized. Further, Kim and Bullard [7] found that fin pitch is independent of heat transfer coefficient, and pressure drop is negatively correlated with fin pitch by conducting an experimental study with the Reynolds number of 100~600. Qi *et al*. [8] concluded the contribution ratios of different factors by Taguchi methodology based on the database from Kim and Bullard [7], and believed that the ratio of fin pitch to fin thickness is a very important factor. Hsieh and Jang [9] found the optimal parameter combination by Taguchi method, in which the fin pitch and louver angle are assigned to 2.1 mm and 36°, respectively. Erbay *et al*. [10] conducted that the effects of fin pitch are greater than that of louver angle, and provided the optimal geometry at Re = 229 with the louver angle of 20° and fin pitch of 1.5 mm. Javaherdeh *et al*. [11] conducted the investigation for the different louver angles varying from 12° to 60° by ε-NTU method. The heat transfer rate can reach a maximum with the louver angle of 28°, and the proper louver angle stands in the region from 24° to 32°. Qian *et al*. [12] provided an optimal value of 8° for louver angle at a constant 2.06 mm fin pitch, and the comprehensive performance is improved by 19%. Sadeghianjahromi *et al*. [13] concluded that the *j*-factor first increases, then decreases, and finally increases as the angle increases for different fin pitches varying from 2.5-5.0 mm, and the optimal louver angle is about 20° according to the maximum *j*-factor and the minimum *f*-factor. It can be found that different studies have different evaluation criteria, and the traditional optimal angle cannot be extended to other occasions.

To the best of the author's knowledge, Nakayama and Xu [14] conducted the earliest experimental research on slit fin, and proposed the correlations according to the test results of three samples. However, Garimella *et al*. [15] believed that the aforementioned correlations from Nakayama and Xu [14] have a narrow application range. Further, Wang et al. [16, 17] and Du and Wang [18] studied the effects of geometric factors and fitted the correlations. The aforementioned correlations can reflect the strong interaction for fin pitch and slotted height. Yun and Lee [19] established eighteen kinds of scaled-up models by Taguchi methodology, and considered that the fin pitch has the most effect on thermal hydraulic performance. Meanwhile, Wang and Ouyang [20] concluded that the fin pitch has most significant effect on the thermal-hydraulic performance for the ring-bridge slit fin. Zhi *et al*. [21] conducted the numerical simulation on slit fin with small diameter at a constant slotted height, and considered that the largest contribution to *j*-factor is fin pitch and number of tube rows at low Reynolds and high Reynolds numbers, respectively. Further, Zhi *et al*. [22] independently studied the effects of slotted height and fin pitch, and provided the correlations. However, the function between fin pitch and slotted height has not been explored. Even though the longitudinal vortex generator has been put into research and application recently [23, 24], there is still no research indicating the function between fin pitch and slotted height.

It is well known that the optimal angle or slotted height is different under different fin pitches. This paper takes the slotted width as a fixed value, tries to define the slotted height of the louver fin according to the meaning of the slotted height of the slit fin, and explores the interaction function between the slotted height and the fin pitch, so as to find a proper ratio to guide the design of heat exchanger. Hence, a 3-D numerical simulation is carried out to investigate the effects of slotted height at different fin pitches and different Reynolds numbers. Combined with the distributions of velocity, streamline and temperature, the variations of heat transfer coefficient and pressure drop with the slotted height are analyzed in detail under different fin pitches. Taking the maximum comprehensive performance as the objective, the function and optimal ratio of slotted height to fin pitch are obtained, which can provide theoretical support for engineering design.

Model description

Configuration and meshing

The configurations including louver fin and slit fin are presented in fig. 1, in which the red point is the origin of the co-ordinate. The tube pitches in transverse and longitudinal are 13.5 mm and 13.56 mm, respectively. The collar diameter is 5.19 mm, which is the sum of the tube outside diameter and twice fin thickness, δ_f. The slotted widths, S_w, in louver fin and slit fin are 1.3 mm and 1.2 mm, respectively. This paper takes the slotted width as a fixed value, tries to define the slotted height of the louver fin according to the meaning of the slotted height of the slit fin, and explores the optimal proportion and interaction function between the slotted height and the fin pitch. The definitions in the slotted height, S_h, and fin pitch, F_p, can be seen in Detail A and Detail B.

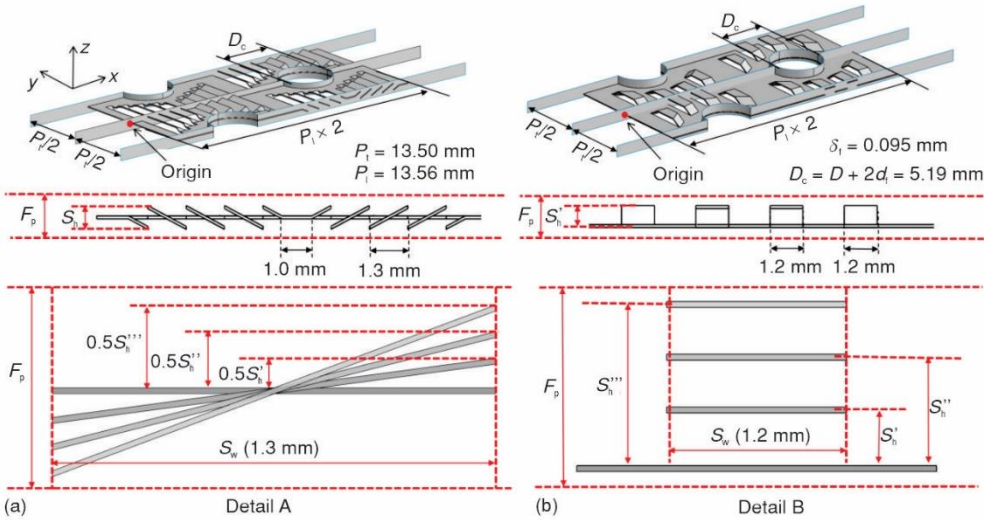

Figure 1. Configurations of the louver fin and slit fin in finned tube heat exchanger; (a) louver fin and (b) slit fin

The air in the domain flows along the *x*-axis direction, and symmetry and periodicity are assigned to the *y*-axis and *z*-axis, respectively. In order to save computing consumption, the computational domain is defined as shown in fig. 2, in which the height is a fin pitch and the length includes the louver/slit fin and the extensions. The minimal flow area will be generated between two adjacent tubes in the same row, and the flow velocity here is the maximum, as shown in fig. 2. The upstream extension and downstream extension are 0.75 times and 4 times of the longitudinal tube pitch, respectively, which can eliminate the effects of inlet and outlet. Table 1 exhibits the boundary conditions. The temperature of tube wall is 321.15 K, and the fin temperature is solved by conjugate [25-27], which is determined by the wall tube temperature and the air temperature. The inlet and outlet are set as the velocity inlet and pressure outlet, respectively, and the air inlet temperature is 293.15 K, the velocity varies from 1.0 m/s to 4.2 m/s. Li *et al.* [28] concluded that under different fluid physical properties, the Nusselt number and friction factor are almost the same at the same Reynolds number. It can be considered that the physical properties in the computational domain are constant. Hence, the physical properties in this paper are at the pressure of 0.101 MPa and temperature of 303.61 K, which are obtained by Refprop 9.1 as shown in tab. 2.

Table 1. Boundary conditions

u_{in} [ms^{-1}]	p_{out} [Pa]	T_{in} [K]	$T_{wall\text{-}tube}$ [K]	Wall-top and bottom	Wall-left and right
Velocity inlet	Pressure outlet				
1.0-4.2	0	293.15	321.15	Periodic	Symmetry

Table 2. The physical properties

Name	Density, ρ	Specific heat, c_p	Thermal conductivity, λ	Dynamic viscosity, μ
Unit	[kgm^{-3}]	[kJkg^{-1}K^{-1}]	[Wm^{-1}K^{-1}]	[Pa·s]
Value	1.1589	1.0068	0.0263	1.8753×10^{-5}

The grid strategies around the tubes and fin surface can be presented in fig. 2. Hexahedral grid is employed for upstream and downstream extensions, and tetrahedral grid is employed for fin coil area. It is necessary to have the grid independence for the better accuracy of the computations. The grid independence can be performed by the grid convergence index (GCI) method proposed by Roache [29], which is a method of minimizing the error of discrete equation solutions through grid refinement. Three sets of grids are assigned to the louver fin to eliminate the effect of grid density on numerical result as shown in tab. 3, in which the slotted height, S_h, is 0.65 mm and the fin pitch, F_p, is 1.2 mm as a representative. The GCI for the three levels of grid refinements can be calculated by follows [30]. The f_i is the discrete solution under different grid strategies, including f_1, f_2 and f_3:

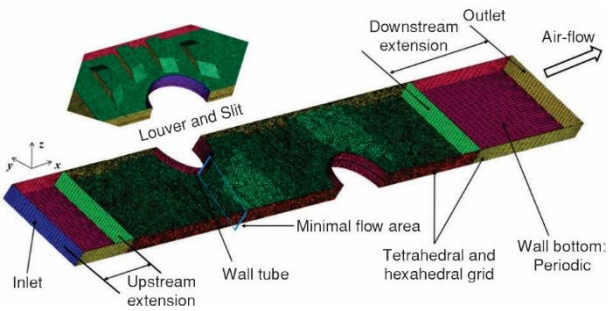

Figure 2. The computational domain and meshing

$$\mathrm{GCI}_{i+1,i} = \frac{F}{\left(r_{i+1,i}^{p}-1\right)}\left|\frac{f_{i+1}-f_i}{f_i}\right| \tag{1}$$

where F_s is the factor of safety, with a value of 1.25. The $r_{i+1,i}$ and p are the grid refinement ratio and order of accuracy, respectively, which can estimated by:

$$r_{i+1,i} = \left(\frac{N_i}{N_{i+1}}\right)^{1/3} \tag{2}$$

$$\frac{f_3-f_2}{\frac{p}{3\,2}\;1} = \frac{r_{2,1}^{p}\left(f_2-f_1\right)}{r_{2,1}^{p}-1} \tag{3}$$

where N_i is the number of grids in the computational domain, including N_1, N_2 and N_3. Small value of GCI indicates that the grids have achieved the convergence range, and the convergence range α of the solution should be close to 1, which can be calculated [30]:

$$\alpha = r_{2,1}^{p}\left(\frac{\mathrm{GCI}_{2,1}}{\mathrm{GCI}_{3,2}}\right) \tag{4}$$

Grid convergence calculations using GCI methods are carried out for all three levels of grid refinements are presented in tab. 3. For all the variables, the value of p is always greater than 0, which indicates that the convergence condition is monotonic convergence [31].

Meanwhile, the value of α in all cases is very close to 1, which also indicates that monotonic convergence has been achieved. In addition, it can be found that the heat transfer coefficient and pressure drop have no obvious variety at all grid densities, and the errors are all at very low levels. Hence, in order to ensure the accuracy of the numerical model and save calculation consumption, the second grid density (846677) is selected as the final scheme.

Table 3. Verification of grid density independence

i	N_i	f_i	Error [%]	$r_{i+1,i}$	$f_{i+1} - f_i$	$GCI_{i+1,i}$	α	p
For Re = 600, h [Wm^{-2}K^{-1}]								
1	1490548	112.295	0.19%	1.073	0.216	0.005	1.002	6.032
2	1205219	112.511	0.57%	1.125	0.643	0.007		
3	846677	113.154						
For Re = 600, Δp [Pa]								
1	1490548	28.090	0.47%	1.073	0.132	0.062	1.005	1.272
2	1205219	28.222	0.88%	1.125	0.247	0.068		
3	846677	28.470						
For Re = 2400, h [Wm^{-2}K^{-1}]								
1	1490548	186.861	0.5%	1.073	0.941	0.028	1.005	2.831
2	1205219	187.802	1.09%	1.125	2.049	0.034		
3	846677	189.851						
For Re = 2400, Δp [Pa]								
1	1490548	228.202	0.37%	1.073	-0.834	0.050	0.996	1.238
2	1205219	227.368	0.69%	1.125	-1.559	0.055		
3	846677	225.809						

Data reduction

According to the conservation of heat transfer:

$$Q = c_p \dot{m}\left(T_{\text{out}} - T_{\text{in}}\right) = h\left(A_{\text{tube}} + A_{\text{fin}}\eta\right)\Delta T_{\log} \tag{5}$$

where $\Delta T_{\log}$ is the logarithmic mean temperature difference and η is the fin efficiency, which can be calculated:

$$\Delta T_{\log} = \frac{\left(T_{\text{w}} - T_{\text{in}}\right) - \left(T_{\text{w}} - T_{\text{out}}\right)}{\ln\dfrac{T_{\text{w}} - T_{\text{in}}}{T_{\text{w}} - T_{\text{out}}}} = \frac{T_{\text{out}} - T_{\text{in}}}{\ln\dfrac{T_{\text{w}} \quad T_{\text{in}}}{T_{\text{w}} \quad T_{\text{out}}}} \tag{6}$$

$$\eta = \frac{Q}{Q_{\text{ideal}}} \tag{7}$$

where the Q_{ideal} is determined by $T_{\text{fin}} = T_{\text{tube}}$ in simulation.

Reynolds number, Nusselt number, Colburn factor-j, friction factor-f, and performance evaluation criteria (PEC) are defined as [32]:

$$\text{Re} = \frac{\rho u_{\max} D_c}{\mu} \tag{8}$$

$$\mathrm{Nu} = \frac{hD_c}{\lambda} \tag{9}$$

$$j = \frac{\mathrm{Nu}}{\mathrm{RePr}^{1/3}} \tag{10}$$

$$f = \frac{2\Delta p}{\rho u_{\max}^2} \frac{A_c}{\left(A_{\mathrm{tube}} + A_{\mathrm{fin}}\right)} \tag{11}$$

$$PEC = j / f^{1/3} \tag{12}$$

where the $u_{\max}$ is the maximum velocity that can be calculated by conservation of mass, which is located at the minimum flow area in fig. 2 [33].

Governing equations and model validation

The FLUENT 19.0 is employed to establish the numerical model. In this paper, the temperature and pressure are extracted from numerical simulation based on area-weighted average. The following is the continuity, momentum, and energy governing equations. The flow is assumed to be incompressible with constant property and the air-flow is steady. The viscous dissipation and gravity are neglected in this paper:

Continuity equation

$$\frac{\partial\left(\rho u_i\right)}{\partial x_i} = 0 \tag{13}$$

Momentum equation

$$\frac{\partial\left(\rho u_i u_k\right)}{\partial x_i} = \frac{\partial}{\partial x_i}\left(\mu \frac{\partial u_k}{\partial x_i}\right) - \frac{\partial p}{\partial x_k} \tag{14}$$

Energy equation

$$\frac{\partial\left(\rho u_i T\right)}{\partial x_i} = \frac{\partial}{\partial x_i}\left(\frac{\lambda}{c_p}\frac{\partial T}{\partial x_i}\right) \tag{15}$$

The velocity and Reynolds number in this paper are low and the laminar model should be adopted to solve the numerical model. Meanwhile, the laminar model has been adopted in simulations of louver fin [34, 35] and slit fin [24]. The simulation results by laminar model are compared with the experimental correlations [16, 36], as shown in fig. 3. The parameters for model validation are shown in tab. 4. Although there are some inconsistencies between the parameter ranges in literature and the parameter ranges in this study, the simulation model of the same size as that in literature is established and the calculations are carried out. For louver fin, the mean error of h is 2.94% and the mean error of Δp is only 1.32% within the entire velocity range. For slit fin, the mean error of h is 7.87% and the mean error of Δp is only 0.63% within the entire velocity range. The laminar model is consistent strongly with the experimental data within the entire velocity range, and the main errors come from the simplification of the numerical model. For example, a constant temperature is given to the wall tube in numerical simulation, which is only close to the constant in practice. In addition, there is no air passing through the symmetry, but it will occur in practice. Finally, convergence error of numerical simulation and measurement error of experiment will also contribute. Moreover, [34] summarized that even if it is noted that there is the error between CFD simulations and experimental results, the trend in CFD simulation is comparable.

Table 4. Parameters for model validation in literatures [16, 36]

Parameters	N	P_t	P_l	F_p	N_s	S_h	S_w	δ_f
Unit	–	[mm]	[mm]	[mm]	–	[mm]	[mm]	[mm]
Louver	1	25.4	19.05	1.915	6	0.9	2.4	0.115
Slit	2	25.4	22	2.48	4	0.99	2.2	0.12

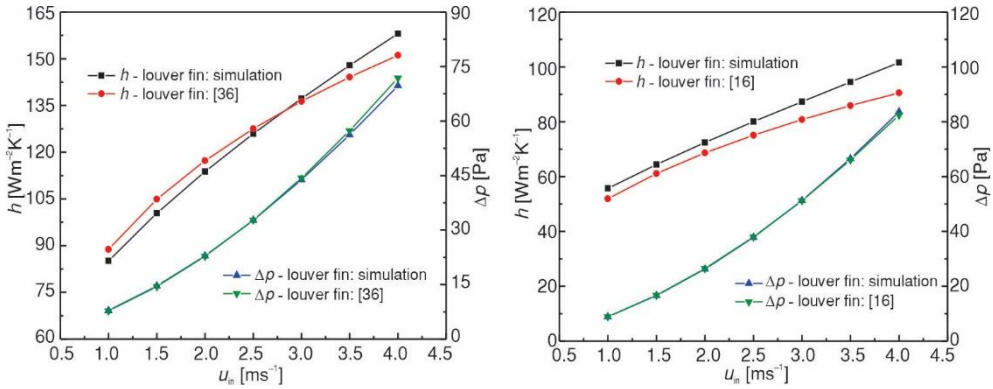

Figure 3. Comparison of *h* and Δ*p* between the present and experimental data

Results and discussion

The effect of slotted height on louver fin performance

It can be observed from fig. 4 that with the increasing S_h, the overall trend of the h at low Reynolds number is to increase first and then decrease. In the cases of high Reynolds number, the *bimodal phenomenon* begins to appear. As the S_h is about half of the F_p, the h has a local minimum value, of which there are two peaks on both sides. It can be mainly explained combined with the distributions of velocity and streamline at y = 0.2 mm. As the S_h is 0.25 mm (F_p = 1.2 mm) or 0.45 mm (F_p = 1.8 mm) shown in fig. 5, the S_h is at a lower level than the F_p, and the air is directed by the fin (duct-directed flow) [10]. As the S_h continues to increase to 0.45 mm (F_p = 1.2 mm) or 0.775 mm (F_p = 1.8 mm), more air is directed by the louvers (louver-directed flow) [10], and the air passing between the two louvers of the upper layer can just scour the louvers of the lower layer, indicating that the h reaches the first peak (Peak-1). As the S_h is 0.65 mm (F_p = 1.2 mm) or 0.9 mm (F_p = 1.8 mm), the upper and lower louvers are geometrically parallel shown in fig. 5, which is falling under Scene-A explained in detail in fig. 6. Further, the air passing through the upper louvers still passes through the lower louvers in parallel. Hence, the heat transfer coefficient has a local minimum. As the S_h continues to increase to 0.85 mm (F_p = 1.2 mm) or 1.25 mm (F_p = 1.8 mm), the geometric parallelism disappears. The air passing between the two louvers of the upper layer can scour the louvers of the lower layer again, and the h reaches the second peak (Peak-2). As the S_h continues to increase to 1.05 mm (F_p = 1.2 mm) or 1.65 mm (F_p = 1.8 mm), the upper and lower louvers are nearly completely parallel, and the h starts to decrease, which is falling under Scene-B explained in detail in fig. 6. Figure 7 shows the temperature distributions of louver fins at y = 0.2 mm. It can be clearly seen that the temperature distribution is roughly consistent with the distribution of heat transfer coefficient. There are still low temperature regions along the flow direction and the air cannot be effectively heated by the fins under duct-directed flow and Scene-B. The low temperature region under Scene-A is also slightly larger than the region at the Peak-1 and Peak-2. In addition,

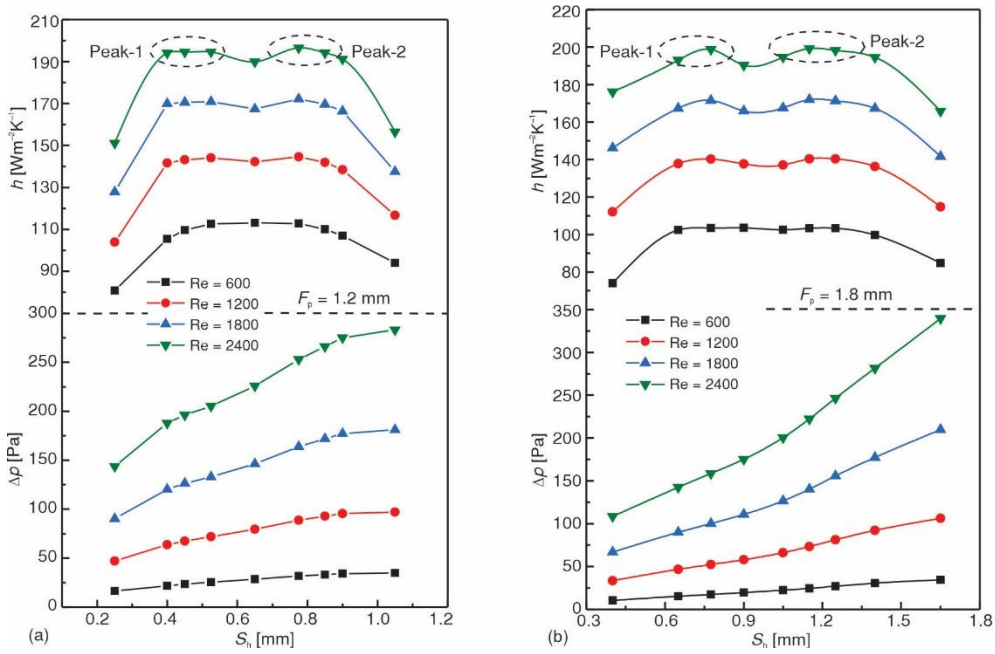

Figure 4. Effects of slotted height on *h* and Δ*p* at different fin pitches for louver fin; (a) F_p = 1.2 mm and (b) F_p = 1.8 mm

during the process of increasing the S_h, the Δp has been increasing. It can be interpreted as that with the increasing S_h, the Δp caused by changing of the flow direction plays a decisive role. It can be seen from fig. 5 that for all cases where the fin pitch is 1.2 mm, the streamline is smooth

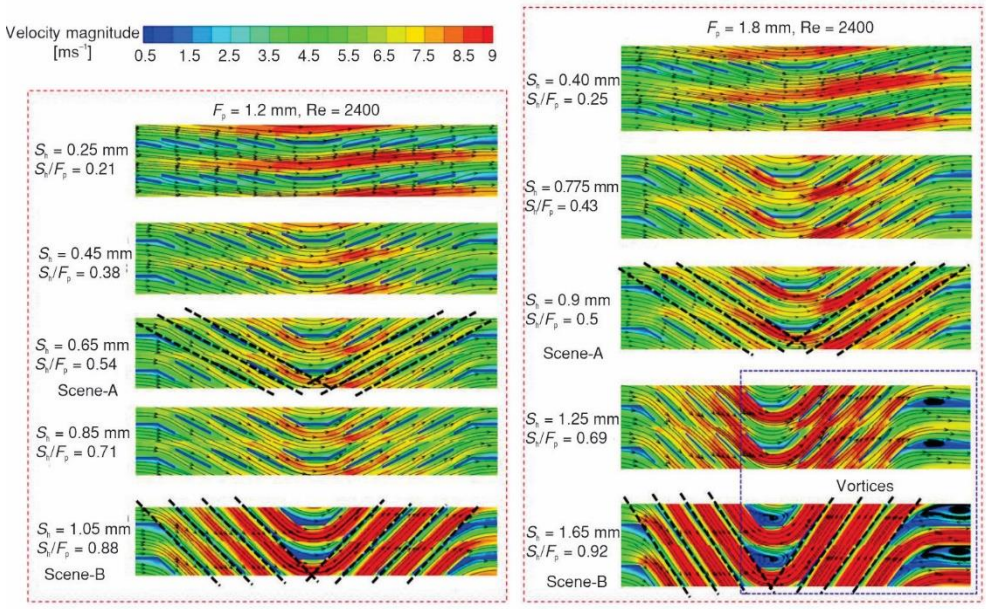

Figure 5. Contours of velocity and streamline at different slotted heights (*y* = 0.2 mm)

and there are no vortices present. For the cases where the fin pitch is 1.8 mm, the streamline is also smooth if the slotted height is less than 0.9 mm. As the slotted height increases to 1.25 mm, a part of the vortex can be clearly seen in the blue box, as shown in fig. 5. Hence, it can be concluded that vortices appear at the larger slotted height and fin pitch, which is easy to cause greater pressure drop shown in fig. 5. According to the geometric relationship, it can be found that the optimal slotted height under different fin pitches is more instructive than the optimal louver angle.

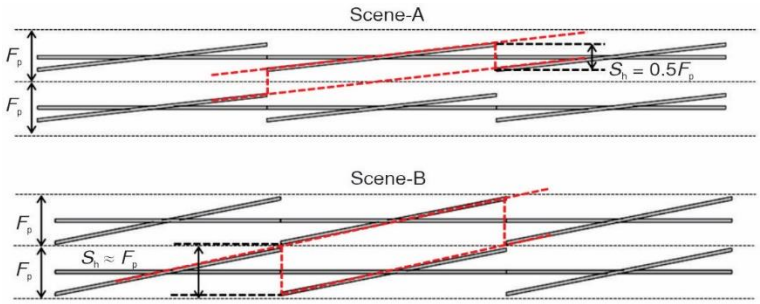

Figure 6. The scenes where the upper louver is parallel to the lower louver

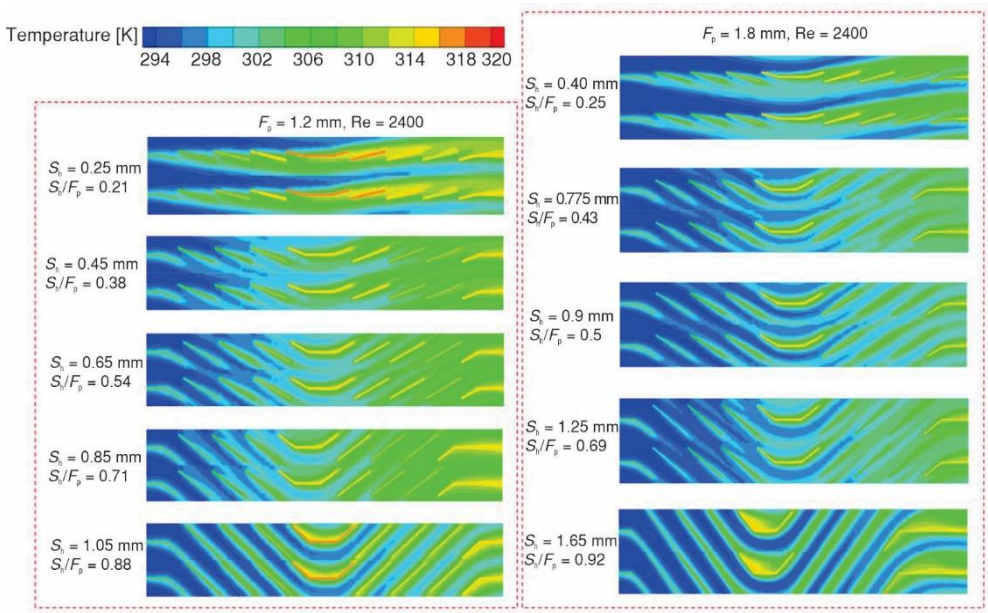

Figure 7. Contours of temperature at different slotted heights and fin pitches (y = 0.2 mm)

The effect of slotted height on slit fin performance

Figure 8 outlines the varieties of the h and Δp under different slotted heights and fin pitches. The h and Δp increase first and then decrease with the increasing slotted height. As the slotted height is half of the fin pitch, the h and Δp can reach the maximum. With the increase of Reynolds number, the slotted height corresponding to the maximum value increases. According to the contours of streamline and velocity at y = 2 mm in fig. 9, it can be interpreted as

follows. As the slotted height is 0.25 mm (F_p = 1.2 mm and F_p = 1.8 mm), which is at a low level. Most of the air passes through the middle of two adjacent fins, and the air cannot effectively scour the slit fin, resulting in the small h and Δp. As the slotted height continues to increase to about half of the fin pitch (S_h / F_p = 0.5), the slit is roughly the same distance from the upper layer and the lower layer fins. Further, the incoming air can form an effective scour and have the largest turbulence intensity in the channel between the two layers of fins, resulting in the largest h and Δp. As the slotted height further increases to 0.9 mm (F_p = 1.2 mm) or 1.6 mm (F_p = 1.8 mm), the slit begins to approach the upper fin. The channel between the upper and lower fins becomes larger, in which most of the air passes through. The air cannot effectively scour the slit fin, indicating that the h and Δp begin to decrease. Figure 10 shows the temperature distributions of slit fins at y = 2 mm. If the slotted height is too large or too small, there will be situations where the air cannot be effectively heated. As the slotted height is about half of the fin pitch (S_h / F_p = 0.5), the air can effectively scour the fins, and the area of the low temperature region along the flow direction is the smallest.

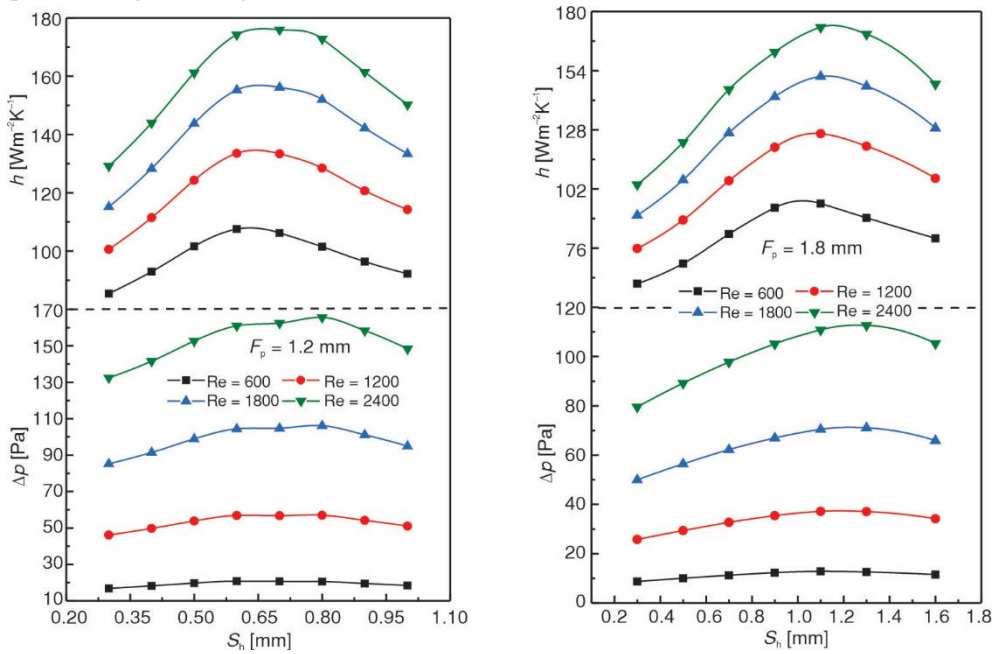

Figure 8. Effects of slotted height on h and Δp at different fin pitches for slit fin; (a) F_p = 1.2 mm and (b) F_p = 1.8 mm

The effect of slotted height on performance evaluation criteria

Figure 11 demonstrates the comprehensive performance for louver fin and slit fin at different fin pitches. First of all, it can be concluded that under different Reynolds numbers, the trend of the PEC with the slotted height is consistent with the trend of the above heat transfer coefficient on the whole. With the increasing Reynolds number, the PEC under the same condition decreases, which is mainly due to the faster increase of the flow resistance compared with the heat transfer coefficient with the increasing Reynolds number. Secondly, as the slotted height is about 0.3~0.45 times of the fin pitch, the PEC of the louver fin can reach the maximum.

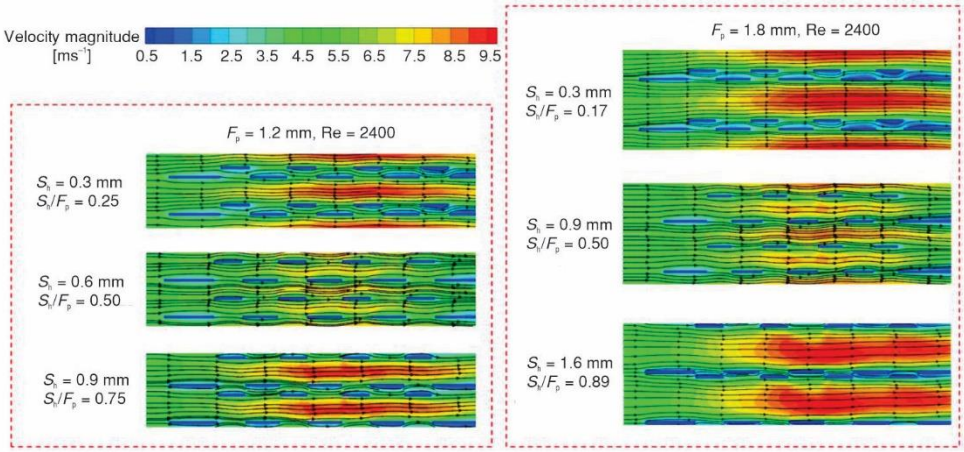

Figure 9. Contours of velocity and streamline at different slotted heights (y = 2.0 mm)

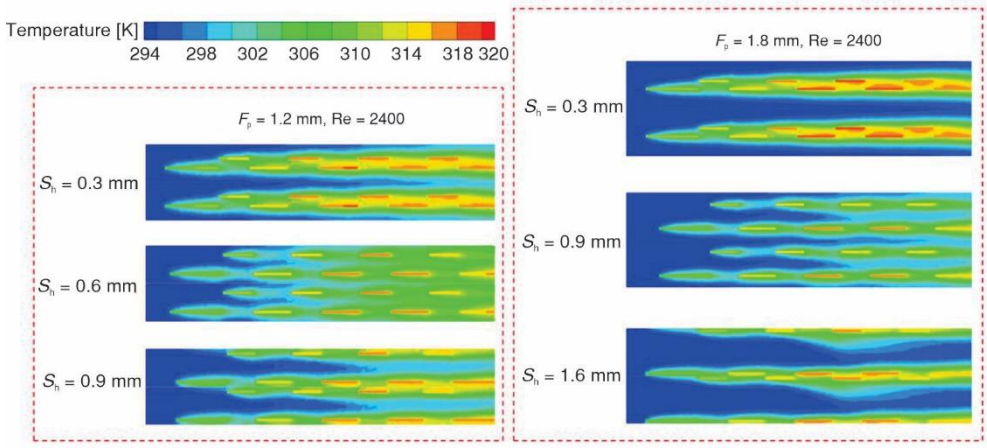

Figure 10. Contours of temperature at different slotted heights and fin pitches (y = 2.0 mm)

And the maximum PEC under 1.2 mm fin pitch is greater than the maximum PEC under 1.8 mm fin pitch. For the slit fin, as the slotted height is about 0.5~0.65 times of the fin pitch, the PEC reaches the maximum. With the increasing Reynolds number, the optimal slotted height will increase slightly. It is same to the louver fin that the maximum PEC under 1.2 mm fin pitch is greater than the maximum PEC under 1.8 mm fin pitch. Meanwhile, it can be seen that the maximum PEC of louver fin is roughly similar to the slit fins for lower Reynolds numbers, which indicates that the increase rate of heat transfer coefficient caused by the change of flow direction is roughly equal to the increase rate of flow resistance. The maximum PEC of louver fin is greater than that of slit fin for higher Reynolds numbers, indicating that the benefit of heat transfer coefficient brought by the change of flow direction is greater than the cost of increasing flow resistance.

Conclusions

The optimal angle or slotted height is different under different fin pitches, and there is no criterion to link the louver angle or slotted height with fin pitch in current research. The-

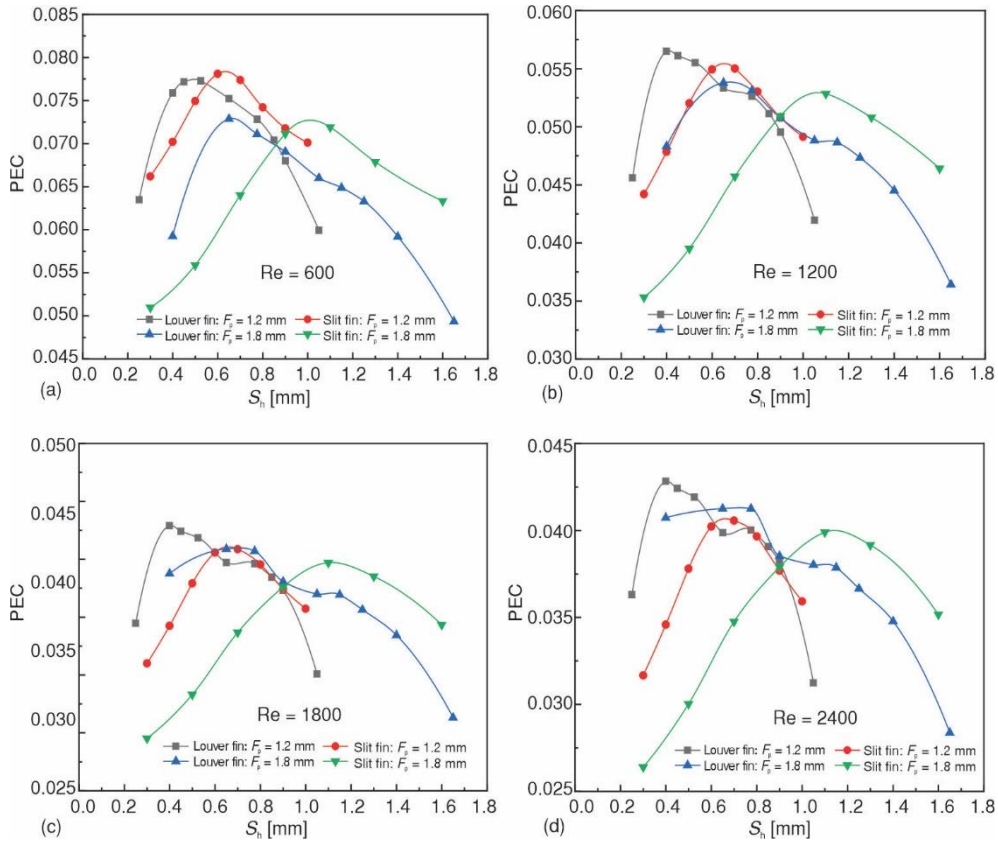

Figure 11. Varieties in PEC with the increasing slotted height at different Reynolds numbers; (a) Re = 600, (b) Re = 1200, (c) Re = 1800, and (d) Re = 2400

refore, this paper tries to define the slotted height of the louver fin according to the meaning of the slotted height of the slit fin, and explores the interaction function between the slotted height and the fin pitch. Combined with the distributions of velocity and streamline, the effects of slotted height on air side performance at different fin pitches for louver fin and slit fin are investigated in detail. The main conclusions are summarized as follow.

- With the increasing slotted height for louver fin, the overall trend of the heat transfer coefficient at low Reynolds number is to increase first and then decrease. In the cases of high Reynolds number, the *bimodal phenomenon* begins to appear. As the slotted height is about half of the fin pitch, the heat transfer coefficient has a local minimum value, of which there are two peaks on both sides. However, the pressure drop has been increasing with the increase of the slotted height. According to the geometric relationship, it can be found that the optimal slotted height under different fin pitches is more instructive than the optimal louver angle.
- In the cases of slit fin, the heat transfer coefficient and pressure drop increase first and then decrease with the increasing slotted height. As the slotted height is half of the fin pitch, the heat transfer coefficient and pressure drop can reach a maximum. With the increase of Reynolds number, the slotted height corresponding to the maximum value increases.
- The comprehensive performance of louver fin and slit fin at different Reynolds numbers is compared. As the slotted height is about 0.3~0.45 times and 0.5~0.65 times of fin pitch for

louver fin and slit fin, respectively, the comprehensive performance can reach a maximum. The maximum PEC under 1.2 mm fin pitch is greater than the maximum PEC under 1.8 mm fin pitch. For lower Reynolds numbers, the optimal comprehensive performance of louver fin is roughly similar to the slit fin. For higher Reynolds numbers, the optimal comprehensive performance of louver fin is greater than that of slit fin.

Nomenclature

A_c – minimal flow area [m^2]
A_o – total surface area [m^2]
A_{total} – total heat transfer area [m^2]
c_p – specific heat [Jkg^{-1}K^{-1}]
D_c – collar diameter [m]
D_o – tube outside diameter [m]
F_p – fin pitch [m]
f – friction factor
h – heat transfer coefficient [W K^{-1}m^{-2}]
$\dot{m}$ – mass-flow rate [kgs^{-1}]
N – number of tube rows
Nu – Nusselt number
P_t – transverse tube pitch [m]
P_l – longitudinal tube pitch [m]
Pr – Prandtl number
p – pressure [Pa]
Δp – pressure drop [Pa]
Q – heat transfer rate [W]
Re Reynolds number
S_h – slotted height [m]
S_w – slotted widths [m]
T – temperature [K]
ΔT_{log} – log mean temperature difference [K]
u velocity [ms^{-1}]

Greek symbols

δ_f – fin thickness [m]
λ thermal conductivity [Wm^{-1}K^{-1}]
ρ density [kgm^{-3}]
μ dynamic viscosity [Pas]
η fin efficiency

Subscripts

in – inlet
out – outlet
max – – maximum
w – wall

Acknowledgment

This work is supported by National Natural Science Foundation of China (Nos. 52006164 and 52276019) and Fundamental Research Funds for the Central Universities (No. xzy012022074).

References

[1] Sahoo, R. R., *et al.*, Performance Comparison of Various Coolants for Louvered Fin Tube Automotive Radiator, *Thermal Science*, *21* (2017), 6B, pp. 2871-2881
[2] Kong, Y. Q., *et al.*, Effects of Continuous and Alternant Rectangular Slots on Thermo-Flow Performances of Plain Finned Tube Bundles in In-Line and Staggered Configurations, *International Journal of Heat and Mass Transfer*, *93* (2016), Feb., pp. 97-107
[3] Sadeghianjahromi, A., Wang, C.-C., Heat Transfer Enhancement in Fin-and-Tube Heat Exchangers – A Review on Different Mechanisms, *Renewable and Sustainable Energy Reviews*, *137* (2021), 110470
[4] Chu, H., *et al.*, Progress in Enhanced Pool Boiling Heat Transfer on Macro- and Micro-Structured Surfaces, *International Journal of Heat and Mass Transfer*, *200* (2023), 123530
[5] Jiang, H., *et al.*, Effect of T-Shaped Micro-Fins on Pool Boiling Heat Transfer Performance of Surfaces, *Experimental Thermal and Fluid Science*, *136* (2022), 110663
[6] Kays, W., London, A., Heat-Transfer and Flow-Friction Characteristics of Some Compact Heat-Exchanger Surfaces: Part 1—Test System and Procedure, *Transactions of the American Society of Mechanical Engineers*, *72* (1950), 8, pp. 1075-1085
[7] Kim, M.-H., Bullard, C. W., Air-Side Thermal Hydraulic Performance of Multi-Louvered Fin Aluminum Heat Exchangers, *International Journal of Refrigeration*, *25* (2002), 3, pp. 390-400
[8] Qi, Z.-G., *et al.*, Parametric Study on the Performance of a Heat Exchanger with Corrugated Louvered Fins, *Applied Thermal Engineering*, *27* (2007), 2, pp. 539-544
[9] Hsieh, C.-T., Jang, J.-Y., Parametric Study and Optimization of Louver Finned-Tube Heat Exchangers by Taguchi Method, *Applied Thermal Engineering*, *42* (2012), Sept., pp. 101-110

[10] Erbay, L. B., *et al.*, Numerical Investigation of the Air-Side Thermal Hydraulic Performance of a Louvered-Fin and Flat-Tube Heat Exchanger at Low Reynolds Numbers, *Heat Transfer Engineering*, *38* (2017), 6, pp. 627-640
[11] Javaherdeh, K., *et al.*, Experimental and Numerical Investigations on Louvered Fin-and-Tube Heat Exchanger with Variable Geometrical Parameters, *Journal of Thermal Science and Engineering Applications*, *9* (2017), 2, 024501
[12] Qian, Z., *et al.*, Simulation Investigation on Inlet Velocity Profile and Configuration Parameters of Louver Fin, *Applied Thermal Engineering*, *138* (2018), June, pp. 173-182
[13] Sadeghianjahromi, A., *et al.*, Optimization of the Louver Fin-and-Tube Heat Exchangers− A Parametric Approach, *Journal of Enhanced Heat Transfer*, *27* (2020), 4, pp. 289-312
[14] Nakayama, W., Xu, L., *Enhanced Fins for Air-Cooled Heat Exchangers—Heat Transfer and Friction Correlations*, 1st ASME/JSME Thermal Engineering Joint Conference, New York, USA, 1983, pp. 495-502
[15] Garimella, S., *et al.*, Tube and Fin Geometry Alternatives for the Design of Absorption-Heat-Pump Heat Exchangers, *4* (1997), 3, pp. 217-235
[16] Wang, C.-C., *et al.*, An Investigation of the Airside Performance of the Slit Fin-and-Tube Heat Exchangers, *International Journal of Refrigeration*, *22* (1999), 8, pp. 595-603
[17] Du, Y.-J., Wang, C.-C., An Experimental Study of the Airside Performance of the Superslit Fin-and-Tube Heat Exchangers, *International Journal of Heat and Mass Transfer*, *43* (2000), 24, pp. 4475-4482
[18] Wang, C.-C., *et al.*, A Comparative Study of Compact Enhanced Fin-and-Tube Heat Exchangers, *International Journal of Heat and Mass Transfer*, *44* (2001), 18, pp. 3565-3573
[19] Yun, J.-Y., Lee, K.-S., Influence of Design Parameters on the Heat Transfer and Flow Friction Characteristics of the Heat Exchanger with Slit Fins, *International Journal of Heat and Mass Transfer*, *43* (2000), 14, pp. 2529-2539
[20] Wang, Z., Ouyang, X., Numerical Simulation of Heat Transfer and Flow Characteristics for Plate Fin-and-Tube Heat Exchanger with Ring-Bridge Slit Fins, *Thermal Science*, 2023, On-line first, https://doi.org/10.2298/TSCI230123096W
[21] Zhi, C., *et al.*, Numerical Investigation of Slit Fin at Different Reynolds Numbers: A Sensitivity Analysis and Optimization by Taguchi Methodology, *International Communications in Heat and Mass Transfer*, *138* (2022), 106393
[22] Zhi, C., *et al.*, Prediction and Analysis of Thermal-Hydraulic Performance with Slit Fins in Small Diameter (3 mm to 4 mm) Heat Exchangers, *International Communications in Heat and Mass Transfer*, *129* (2021), 105684
[23] Li, J., *et al.*, Numerical Study on a Slit Fin-and-Tube Heat Exchanger with Longitudinal Vortex Generators, *International Journal of Heat and Mass Transfer*, *54* (2011), 9, pp. 1743-1751
[24] Moreno, R. R., *et al.*, Numerical Optimization of a Heat Exchanger with Slit Fins and Vortex Generators Using Genetic Algorithms, *International Journal of Refrigeration*, *119* (2020), Nov., pp. 247-256
[25] Zhang, X., *et al.*, Numerical Investigation of the Air-Side Performance of Louver Fin-and-Tube Radiators Having Rectangular, Tapered and Airfoil Section Configuration, *Energy Reports*, *8* (2022), Nov., pp. 11799-11809
[26] Menendez Perez, A., *et al.*, Parametric Analysis of the Influence of Geometric Variables of Vortex Generators on Compact Louver Fin Heat Exchangers, *Thermal Science and Eng. Progress*, *27* (2022), 101151
[27] Yoo, B. K., *et al.*, Numerical Analysis and Correlation of Thermohydraulic Characteristics of Louvered Fin-Tube Heat Exchanger, *International Journal of Refrigeration*, *147* (2022), Mar., pp. 121-133
[28] Li, X.-Y., *et al.*, Numerical Study on the Heat Transfer and Pressure Drop Characteristics of Fin-and-Tube Surface with Four Round-Convex Strips Around Each Tube, *International Journal of Heat and Mass Transfer*, *158* (2020), 120034
[29] Roache, P. J., Perspective: A Method for Uniform Reporting of Grid Refinement Studies, *Journal of Fluids Engineering*, *116* (1994), 3, pp. 405-413
[30] Naik, H., Tiwari, S., Thermal Performance Analysis of Fin-Tube Heat Exchanger with Staggered Tube Arrangement in Presence of Rectangular Winglet Pairs, *International Journal of Thermal Sciences*, *161* (2021), 106723
[31] Eca, L., Hoekstra, M., Evaluation of Numerical Error Estimation Based on Grid Refinement Studies with the Method of the Manufactured Solutions, *Computers & Fluids*, *38* (2009), 8, pp. 1580-1591
[32] Saleem, A., Kim, M.-H., Airside Thermal Performance of Louvered Fin Flat-Tube Heat Exchangers with Different Redirection Louvers, *Energies*, *15* (2022), 16, 5904

[33] Zhi, C., *et al.*, Thermodynamic Assessment and Optimization on Louver Fin with Non-Uniform Arrangement at Different Tube Rows by Desirability Approach, *Thermal Science and Engineering Progress*, *42* (2023), 101899
[34] Perrotin, T., Clodic, D., Thermal-Hydraulic CFD Study in Louvered Fin-and-Flat-Tube Heat Exchangers, *International Journal of Refrigeration*, *27* (2004), 4, pp. 422-432
[35] Čarija, Z., *et al.*, Heat Transfer Analysis of Fin-and-Tube Heat Exchangers with Flat and Louvered Fin Geometries, *International journal of refrigeration*, *45* (2014), Sept., pp. 160-167
[36] Wang, C.-C., *et al.*, Heat Transfer and Friction Correlation for Compact Louvered Fin-and-Tube Heat Exchangers, *International journal of heat and mass transfer*, *42* (1999), 11, pp. 1945-1956

Paper submitted: March 27, 2023
Paper revised: June 3, 2023
Paper accepted: June 14, 2023